12th International Conference on Fracture Mechanics of Concrete and Concrete Structures
FraMCoS-12
B.L.A. Pichler, Ch. Hellmich, P. Preinstorfer (Eds)

https://doi.org/10.21012/FC12.1246
TT-G:1

INFLUENCE OF FIBER REINFORCEMENT ON THE BLAST RESISTANCE AND FRACTURE BEHAVIOR OF HIGH-STRENGTH CONCRETE SLABS

DAVID A. CENDÓN[*], FRANCISCO GÁLVEZ[*], GONZALO RUIZ[†] AND XIAOXIN ZHANG[††]

[*] ETSI Caminos, C. y P. — Universidad Politécnica de Madrid
C/ Profesor Aranguren 3, 28040, Madrid, Spain
e-mail: david.cendon.franco@upm.es | f.galvez@upm.es

[†] ETSI Caminos, C. y P. — Universidad de Castilla-La Mancha
Avda. Camilo José Cela s/n, 13071 Ciudad Real, Spain
e-mail: Gonzalo.Ruiz@uclm.es

[††] Mining and Industrial Engineering School of Almadén — Universidad de Castilla-La Mancha
Plaza Manuel Meca, s/n, 13400 Almadén, Ciudad Real, Spain
e-mail: Xiaoxin.Zhang@uclm.es

Key words: High-performance fiber-reinforced concrete, high strain rates, softening behavior, blast loading.

Abstract: Steel fiber reinforced concrete (SFRC) is an effective material for structures that must endure dynamic events like impacts, earthquakes, and explosions. Recent studies highlight the role of mechanical properties related to fracture in how concrete responds to blast loads. This study examines high-strength SFRC slabs subjected to such loads. Three self-compacting concrete mixes were developed to explore the effects of varying fiber content on structural performance. Concrete A, with low reinforcement, had 40 kg/m³ of 13-mm long fibers. Concrete B and C added 20 kg/m³ and 40 kg/m³ of 30-mm long fibers to concrete A, respectively. Testing showed distinct softening behaviors among the mixes. After blast tests, concrete B had a higher crack density than concrete A due to greater hardening, while concrete C exhibited superior resistance to crack initiation, resulting in fewer cracks. These results demonstrate that higher fiber content enables better energy dissipation through crack propagation and stress redistribution, enhancing the overall performance of the concrete.

1 INTRODUCTION

Terrorist attacks worldwide underscore the vulnerability of civil and transport infrastructure to such threats. Explosions targeting airports, railway and subway stations, bridges, and governmental buildings have resulted in significant damage and loss, particularly when followed by the progressive collapse of entire structures [1,2]. This has led to increased research interest in enhancing the performance of structural materials under impulsive loads [3-5]. Fiber-reinforced concretes (FRCs) have emerged as a promising solution for increasing structural ductility and resilience in concrete structures.

Among FRCs, high-performance fiber-reinforced concretes (HPFRCs) represent a significant advancement, offering improved strength, ductility, and durability compared to traditional and high-performance concrete. These benefits are especially evident under impulsive loading conditions such as impact and blast [3]. HPFRCs are characterized by the incorporation of various types of fibers into a high-strength concrete matrix. Their superior mechanical properties stem primarily from their post-cracking residual strength, which depends on variables such as fiber content, type, geometry,

water-cement ratio, and maximum aggregate size [6].

Despite the demonstrated potential of HPFRCs to enhance structural performance against impulsive loads, limited knowledge exists about their mechanical behavior under high strain rates. Although some experimental studies have explored the behavior of structural members made from HPFRCs under blast and impact conditions [7,8], there is a notable lack of systematic investigations at the material level under high strain rates [9,10].

This paper presents preliminary findings from research aimed at understanding the behavior of HPFRCs under impulsive loads, specifically impact and blast scenarios. Three self-compacting HPFRCs with varying softening behaviors were developed and evaluated. Standard compressive tests were conducted to determine compressive strength, Young's modulus, and Poisson's ratio, alongside fracture energy tests at two distinct strain rates. Additionally, blast tests on slabs made from the three concrete mixes revealed a clear correlation between fiber reinforcement dosage and observed crack patterns.

2 MATERIALS

2.1 Concrete mixes

Three distinct concrete mixes, labeled as A, B, and C, were designed in this research to achieve varying softening behaviors. All three mixes utilized the same high-strength concrete matrix, incorporating steel fibers in different types and proportions. The matrix comprised CEM I 42.5 R-SR cement, silica fume, siliceous filler, fine sand, coarse sand, and water, with their respective weight ratios being 1: 0.12: 0.35: 1.21: 1.27: 0.38.

The variations among the three mixes arose from the type and proportion of steel fibers. Two fiber types were used: straight, short fibers and hooked-end, long fibers. The short fibers (Bekaert OL 13/.20) were 13.0 mm in length, with a diameter of 0.3 mm and an aspect ratio of 65. The long fibers (Bekaert RC 80/30 BP) measured 30 mm in length, with a diameter of 0.38 mm and an aspect ratio of 80. Table 1 summarizes the fiber types and quantities used in each mix.

The workability of the fresh concrete mixes was evaluated using slump flow measurements based on the standard Abrams cone test (Fig. 1). The results, reported as the largest diameters measured in two perpendicular directions, are presented in Table 2.

Table 1: Fiber contents.

Concrete type	Short fiber (kg/m^3)	Long fiber (kg/m^3)
A	40	—
B	40	20
C	40	60

Table 2: Slump test results.

Concrete type	Slump diameters (mm)
A	700 × 700
B	660 × 670
C	570 × 570

Figure 1: Slump test result.

2.2. Mechanical properties

The mechanical properties of the three concrete types were evaluated by measuring compressive strength, tensile strength, and specific fracture energy.

Compressive strength and Young's modulus were determined using four cylindrical specimens for each concrete mix, with dimensions of 150 mm in diameter and 300 mm in height, in accordance with ASTM C39 [11].

Specific fracture energy until a displacement of 3 mm was measured from $100 \times 100 \times 450\ mm^3$ prismatic notched specimens subjected to bending tests, following the RILEM TC 162-TDF guidelines [12]. To assess the effect of loading rate on specific fracture energy, tests were performed at two different velocities: 2.2 µm/s and 22 mm/s [13]. Four specimens were tested for each loading velocity and concrete type.

Table 3 summarizes the mechanical properties obtained during the characterization campaign. The results confirmed the success of the

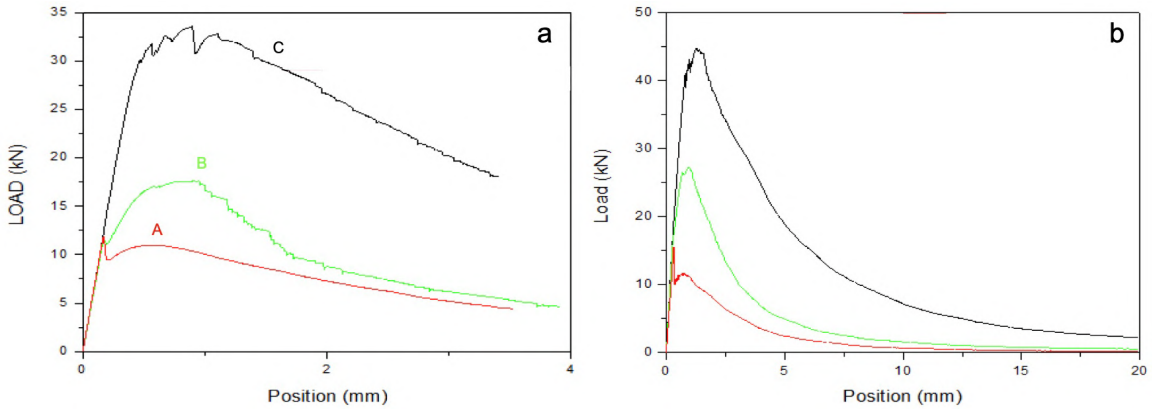

Figure 2: Load-displacement curves for a loading velocity of: a) 2.2 μm/s; b) 22 mm/s.

designed mixes in achieving significantly different softening behaviors. Representative load-displacement curves for the three concretes at both loading rates are shown in Fig. 2.

After the peak load, which corresponds to the onset of fracture, the concrete with the lowest fiber content (A) exhibited a gradual strength reduction with increasing displacement, indicative of softening behavior. In contrast, the mix with the highest fiber content (C) demonstrated greater fracture loads, followed by a hardening phase where strength increased with displacement to a maximum value before gradually decreasing to failure. This hardening behavior is attributed to the higher fiber content, particularly the inclusion of long fibers, which contrasts sharply with the performance of concrete A. The intermediate fiber content (B) resulted in behavior between these two extremes.

Although the behavioral trends were similar for both loading rates, the measured values varied due to the differences in displacement rate.

Table 3: Mechanical properties.

Concrete	G_F at 2.2 μm/s (kN/m)	G_F at 22 mm/s (kN/m)	E (GPa)	ν (–)	f_c (MPa)
A	3.1	3.8	46	0.18	112
B	5.1	6.2	45	0.17	113
C	9.4	12.6	46	0.17	114

2.3 Blast test specimens

Square slabs with dimensions of 500 × 500 × 50 mm^3 were cast using the three previously described concrete mixes. A total of six slabs were produced for each mix, with four slabs from each concrete type selected for blast testing.

3 BLAST TESTS

3.1 General characteristics

The blast tests followed the experimental procedure outlined in [14]. This approach utilized a square steel frame test bench (Fig. 3) capable of accommodating up to four concrete slabs per detonation, ensuring that all samples experienced an identical blast load. The design and dimensions of the steel frame allowed the slabs to be simply supported at their corners, with the explosive pressure uniformly distributed across the slab surface facing the blast.

Figure 3: Test bench used in the tests.

The steel frame had a spacing of 3.00 m between its columns, resulting in a 1.50 m standoff distance from the explosive to the slabs. Additionally, the explosive was positioned 1.70 m above the ground to minimize interference between the direct blast wave and the ground-reflected wave. A schematic of the test bench, including its dimensions, is presented in Fig. 4.

All detonations utilized Goma-2 ECO, a

commercial dynamite-class explosive produced by Maxam. This explosive was supplied in cylindrical cartridges, each containing 151.5 g of explosive material. The TNT equivalent of Goma-2 ECO is approximately 0.9535.

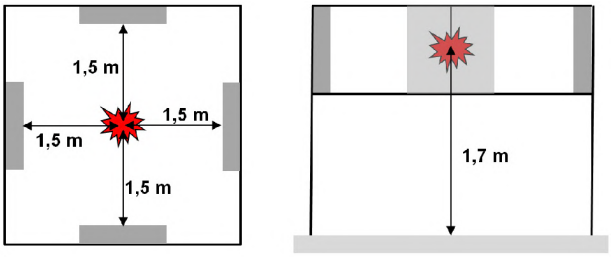

Figure 4: Sketch and dimensions of the test bench.

3.2 Testing procedure

To facilitate a direct comparison of the performance of the three concrete mixes, one slab from each type was included in each detonation. Consequently, three slabs were tested per detonation.

A preliminary test was conducted using 17 cartridges of Goma-2, equivalent to approximately 2.58 kg of explosive, to evaluate the functionality of the data acquisition system and to obtain an initial assessment of the damage caused to the slabs. Since this test produced only limited damage, the explosive load was increased to 22 cartridges, corresponding to 3.322 kg of Goma-2. To address the inherent variability in concrete samples and explosive testing, this test setup was repeated three times, ensuring that three slabs of each concrete mix were subjected to the same blast load. The explosive loads used during the test campaign are summarized in Table 4.

Table 4: Explosive loads and concrete types tested.

Test #	Nº of cartridges	Goma 2 (kg)	TNT eqv. (kg)	A	B	C
1	17	2.58	2.46	1	1	1
2 – 4	22	3.33	3.18	1	1	1

3.3 Blast pressure histories

Blast pressure histories acting on the slabs were recorded during the tests to support subsequent numerical analyses (see Fig. 5). Two PCB Piezotronics 102B piezoelectric pressure gauges were employed for this purpose. The recorded pressure histories demonstrated high consistency across the three tests conducted with 3.33 kg of Goma-2 ECO.

4 RESULTS

4.1 Overall behavior of the slabs

Figure 6 presents the slabs immediately after one of the tests, arranged in order of increasing fiber content from bottom to top. The preliminary results clearly demonstrate the significant influence of fiber content and length on both the fracture patterns and the structural response of the slabs.

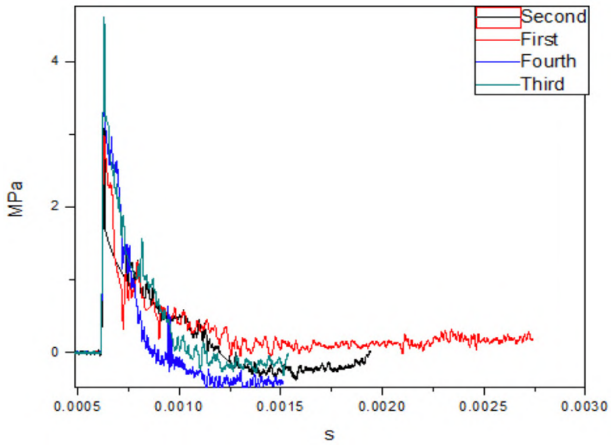

Figure 5: Blast pressure histories.

Figure 6: Slabs after one of the tests. From bottom to top, concretes A, B and C.

In the case of the concrete with the lowest fiber content (Mix A), the energy released through the crack patterns was insufficient to maintain structural integrity, resulting in the detachment of some concrete fragments. Conversely, the concrete with the highest fiber content (Mix C), which included longer fibers and a higher overall fiber dosage, exhibited minimal visible cracks on the tensioned surface, while

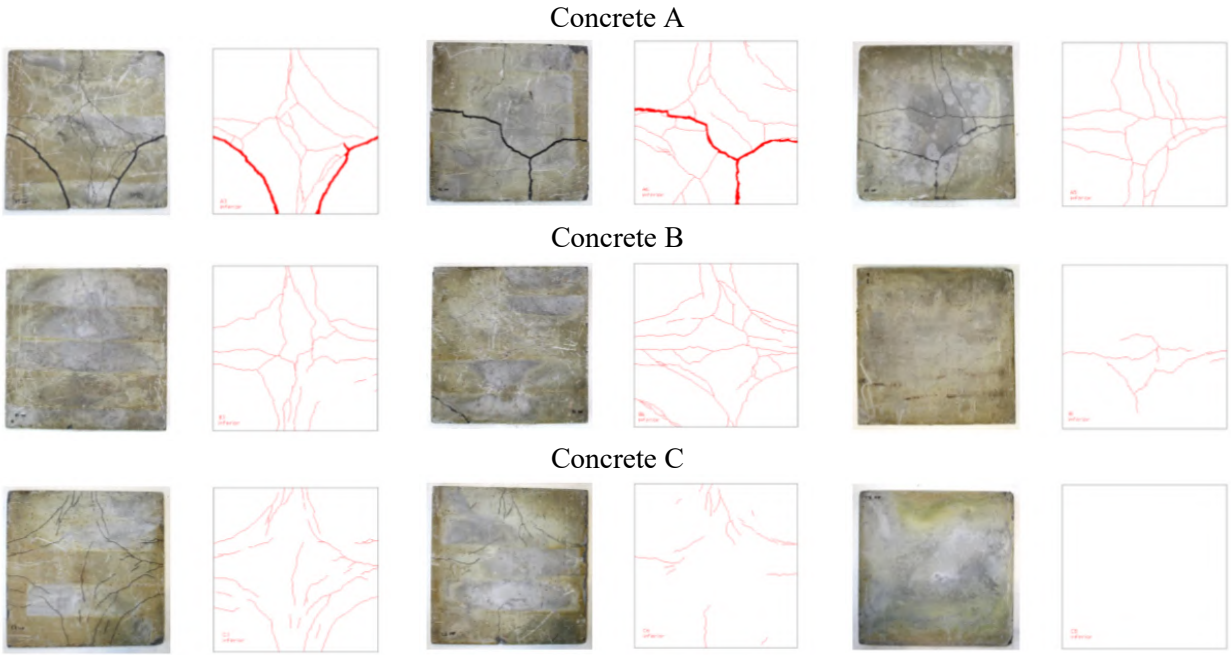

Figure 7: Crack trajectories registered after the tests.

the opposite face remained seemingly undamaged. The concrete with intermediate fiber content (Mix B) displayed a failure behavior between these two extremes, with clearly visible crack patterns that nonetheless preserved the slab's structural integrity.

4.2 Failure patterns

The failure patterns observed after the tests were carefully documented (see Fig. 7). In general, the crack trajectories indicated a dominant trend toward shear failure, characterized by curved cracks around the supports.

Compared to previous experimental campaigns conducted by the authors with fiber-reinforced concretes containing lower fiber contents [15], the concretes tested in this study exhibited significantly more distributed cracking patterns. Figure 8 compares the crack patterns from the current experimental campaign with those from [15]. While the blast loads and self-compacting fiber-reinforced concrete materials were similar in both campaigns, the earlier study utilized 0.7 kg/m³ of long fibers, whereas the present study employed a minimum fiber content of 40 kg/m³. Beyond the evident differences in strength, the increased fiber content induced a strain-hardening behavior that facilitated the redistribution of stresses, enabling the formation of cracks over wider slab areas.

A comparison of the crack patterns between concretes A and B reveals a higher density of cracks in the latter. This observation is likely attributed to the more pronounced hardening behavior of fiber concrete B relative to A (see Fig. 2a). Although both fiber concretes exhibited comparable resistance to crack initiation (as indicated by the peak load in the linear branch of the load-displacement curve), the strength of concrete B increased with displacement, unlike concrete A. In the case of concrete C, its higher resistance to crack initiation (also visible in Fig. 2a) explains the lower crack density observed in the slabs after the blast tests.

These findings highlight the ability of the tested concretes to dissipate substantial amounts of energy through crack propagation. The higher specific fracture energies exhibited by these concretes, coupled with the redistribution of stresses, promoted the creation of new crack surfaces, thereby increasing the total energy dissipation.

5 CONCLUSIONS

This paper presented preliminary findings from research focused on characterizing the behavior of high-performance self-compacting concrete reinforced with steel fibers under impulsive loading.

Three distinct fiber-reinforced concretes, designated as A, B, and C, were developed and subjected to mechanical characterization,

including fracture energy evaluation at two different strain rates. The results demonstrated the effectiveness of the designed mixes, as the concretes exhibited significantly different post-cracking behaviors, confirming the success of the dosage strategy.

Blast tests conducted on slabs made from these concretes revealed a clear influence of fiber shape and content on the observed crack patterns and structural response. The post-cracking behavior of the concretes played a crucial role in the formation and distribution of cracks during the tests, highlighting the importance of fiber reinforcement in enhancing the structural integrity of concrete under blast loads.

We will soon present the results of static and dynamic tests conducted to evaluate the residual strength of the tested slabs. Residual strength is a crucial factor in preventing progressive collapse, which is a primary cause of fatalities and injuries in concrete structures exposed to explosive attacks.

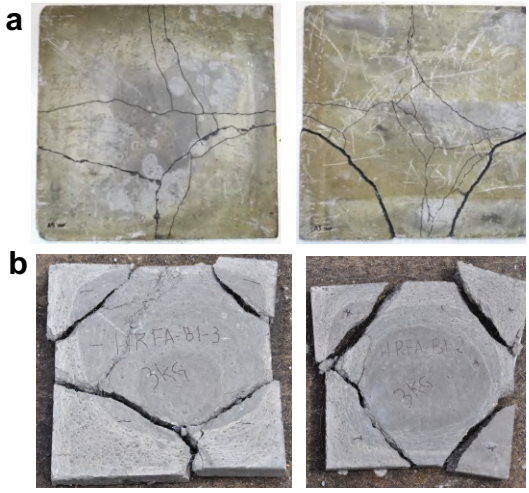

Figure 8: Crack patterns obtained in the tests conducted: a) in concrete A; b) similar slab in [15].

ACKNOWLEDGEMENTS

The authors acknowledge funding from the *Ministerio de Ciencia e Innovación* for projects PID2019-110928RB-C31 and PID2023-147971OB-C31, as well as from the *Universidad de Castilla-La Mancha*, Spain, and the *Fondo Europeo de D. Regional* through grant 2022-GRIN-34124.

REFERENCES

[1] B. Ellingwood, 2006. Mitigating Risk from Abnormal Loads and Progressive Collapse, *J. Perform. Constr. Facil.* **20**, pp. 315–323.

[2] D.O. Dusenberry, 2010. Handbook for Blast Resistant Design of Buildings. John-Wiley & Sons.

[3] Rizwanullah, U.K. Sharma, 2022. Blast loading effects on UHPFRC structural elements: a review. *Innovative Infrastructure Solutions* **7**:341.

[4] R. Castedo, A.P. Santos, A. Alañón, C. Reifarth, M. Chiquito, L.M. López, S. Martínez-Almajano, A. Pérez-Caldentey, 2021. Numerical study and experimental tests on full-scale RC slabs under close-in explosions. *Engineering Structures* **231**: 111774.

[5] T.T. Garfield, W.D. Richins, T.K. Larson, C.P. Pantelides, J.E. Blakeley, 2010. Performance of RC and FRC wall panels reinforced with mild steel and GFRP composites in blast events. *Procedia Eng*, **10**:3534–3539.

[6] T.E.T. Buttignol, J.L.A.O. Sousa, and T.N.Bittencourt, 2017. Ultra High-Performance Fiber-Reinforced Concrete (UHPFRC): a review of material properties and design procedures. *IBRACON Structures and Materials Journal* **10**:957-971.

[7] M. Foglar, R. Hajek, J. Fladr, J. Pachman, J. Stoller, 2017. Full-scale experimental testing of the blast resistance of HPFRC and UHPFRC bridge decks. *Construction and Building Materials* 145:588-601.

[8] J. Xu, C. Wu, H. Xiang, Y. Su, Z-X. Li, Q. Fang, H. Hao, Z. Liu, Y. Zhang, J. Li, 2016. Behaviour of ultra high performance fibre reinforced concrete columns subjected to blast loading. Engineering Structures 118: 97-107.

[9] P Bibora, M Drdlová, V Prachař and O Sviták, 2017. UHPC for Blast and Ballistic Protection, Explosion Testing and Composition Optimization. *Materials Science and Engineering* **251**:012004.

[10] X.X. Zhang, G. Ruiz, M. Tarifa, D. Cendón, F. Gálvez, W.H. Alhazmi, 2017. Dynamic Fracture Behavior of Steel Fiber Reinforced Self-Compacting Concretes (SFRSCCs). *Materials* 10:1270

[11] ASTM C39-02. Standard test method for compressive strength of cylindrical concrete specimen. Annual Book ASTM Standards, 2002.

[12] RILEM. Test and design methods for steel fiber reinforced concrete-Bending test. Materials and Structures, **18**, pp. 285-290, 1985.

[13] X.X. Zhang, G. Ruiz, R.C. Yu and M. Tarifa, 2009. Fracture behaviour of high strength concrete at a wide range of loading rates. Int. J. of Impact Eng. **36**:1204-1209.

[14] G. Morales-Alonso, D.A. Cendón, F. Gálvez, B. Erice, V. Sánchez-Gálvez, 2011. Blast Response Analysis of Reinforced Concrete Slabs: Experimental Procedure and Numerical Simulation. *J. of App. Mech*. **78**:051010.

[15] M. Oña, G. Morales-Alonso, F. Gálvez, V. Sánchez-Gálvez and D.A. Cendón, 2016. Analysis of concrete targets with different kinds of reinforcements subjected to blast loading. *The European Physical Journal*. **225**:265–282.